Proceedings of the International Gas Turbine Congress 2003 Tokyo
November 2-7, 2003

IGTC2003-TS-059

The SST Turbulence Model with Improved Wall Treatment for Heat Transfer Predictions in Gas Turbines

Florian MENTER[1], Jorge CARREGAL FERREIRA[1], Thomas ESCH[1], and Brad KONNO[2]

[1] ANSYS CFX Germany
Staudenfeldweg 12, D-83624 Otterfing, GERMANY
Phone: +49-8024-905415, FAX: +49-8024-905417, E-mail: florian.menter@cfx-germany.com

[2]CFX Asia Pacific K.K.

ABSTRACT

Heat transfer is of key importance in many gas turbine components. Most of the CFD development in this area is focused on advanced turbulence model closures including second moment closure models, and so called Low-Reynolds (low-Re) number and two-layer turbulence models. However, in many cases CFD heat transfer predictions based on these standard models still show a large degree of uncertainty, which can be attributed to the use of the ε-equation as the turbulence scale equation and the associated limitations of the near wall treatment. The present paper demonstrates that an optimally formulated two-equation model in combination with advanced wall treatment can overcome many problems of previous models. The SST (Shear Stress Transport) model in combination with an automatic wall treatment and a model for transition from laminar to turbulent flow was implemented in CFX-5 and applied to different test cases. In all cases the SST model shows to be superior, as it gives more accurate predictions and is less sensitive to grid variations.

NOMENCLATURE

Symbols

c_p	[-]	Specific heat
h	[W/m^{2}K]	Heat-transfer coefficient
k	[W/mK]	Thermal conductivity
k	[m^2/s^2]	Turbulent kinetic energy
Nu	[-]	Nusselt number
Pr	[-]	Prandtl number
q	[W/m^2]	Heat flux
T	[K]	Temperature
u^+	[-]	Non-dimensional velocity
u_τ	[m/s]	Friction velocity
y^+	[-]	Non-dimensional wall distance
κ	[-]	Von Karman Constant
μ	[kg/ms]	Viscosity
τ	[N/m^2]	Wall shear stress
ω	[1/s]	Specific dissipation rate

Subscripts

log	logarithmic region
t	total
vis	viscous region
w	wall

INTRODUCTION

Heat transfer plays a major role in many devices in gas turbines, such as combustion chambers, gas turbine blade cooling, and heat exchangers. Because of its importance, a significant number of CFD methods and analyses for heat transfer predictions have been published for example by Craft et al. (1993), Leschziner (1995), and Dol and Hanjalic (1997). Many of these publications have focused on the development of advanced turbulence model closures including second moment closure models for the turbulent stress tensor and the turbulent heat flux vector. In addition, a large number of so called Low-Reynolds (low-Re) number and two-layer turbulence models have been developed and validated against experimental data. In spite of these efforts, improvements regarding accurate predictions of heat transfer in general industrial devices have been limited to very specific applications and in many cases CFD heat transfer predictions based on standard models still show a large degree of uncertainty.

In addition to the closure level, there are other elements of the turbulence model formulation, which have significant impact on the accuracy of heat transfer simulations. In particular, the near-wall treatment and the turbulence scale equation are of importance (Menter and Esch, 2001). Common in most previous work, the applied turbulence models are based on the ε-equation, a transport equation for the dissipation of the turbulent kinetic energy. As the wall boundary condition there is the choice between wall functions (Viegas and Rubesin, 1983) or integration to the surface using a low Reynolds number (low-Re) formulation (Jones and Launder, 1972). Numerical control of the stability and implementation of this equation close to a wall is difficult and in many cases is the source for numerical instability and model inaccuracy. In addition, these models over-predict the turbulence length scale in flows with adverse pressure gradients which in turn results in high wall shear stress and high heat transfer rates, as shown by Rodi and Scheuerer (1986).

An alternative to the ε-equation is the ω-equation as developed by Wilcox (1993). The ω-equation has significant advantages near the surface and accurately predicts the turbulent length scale in adverse pressure gradient flows, leading to improved wall shear stress and heat transfer predictions. Furthermore, the model has a very simple low-Re formulation, which does not require additional non-linear wall damping terms like it is the case for low-Re k-ε models. However, as shown by Menter (1992) the main deficiency of the standard k-ω model is the strong sensitivity of the solution to free stream values for ω outside the boundary layer. In order to avoid this problem, an optimally formulated two-equation model,

Manuscript Received on April 9, 2003

the SST (Shear-Stress-Transport) model (Menter, 1994) has been proposed. The SST model combines the k-ω model near the wall and the k-ε model away from the wall as a unified two-equation turbulence model. Originally, it was developed for external aerodynamic flow simulations and has shown to be superior to standard k-ε and k-ω models in view of separation, lift, and drag prediction.

In combination with the SST model, an improved near wall treatment will be presented, which gradually switches from a classical low-Re formulation on fine grids to a log-wall function formulation on coarser meshes. This automatic switch of the wall function formulation reduces the stringent grid resolution requirements of the standard low-Re number turbulence models. Recent experience from many different test cases shows that the reduction of the sensitivity of the results to the near wall grid spacing is essential for a successful application of the method to complex industrial flows, where a fine near wall grid can usually not be ensured for all walls in the domain.

Another important element of heat transfer predictions is the transition from laminar to turbulent flow. The transition process can have an important effect on the wall temperature distribution of devices operating at relatively low-Re numbers, like gas turbine blades. Usually, the simulations are carried out as "fully turbulent", with the turbulent boundary layer starting at the nose region of the blade, or the leading edge of a plate. In reality, there can be a substantial portion of laminar flow, with significantly lower heat transfer rates. Some attempts have been made to predict this phenomenon with the help of low-Re k-ε turbulence models such as by Savill (1993). However, the conclusion is that low-Re models alone are not capable to accurately model transition.

An alternative is the use of methods, based on experimental information as correlations (Mayle, 1991, Abu-Ghannam and Shaw, 1980). While these models are more reliable, they have the disadvantage that their formulation is based on non-local variables. Non-local variables are variables that cannot be computed on a cell-by-cell basis (e.g.: momentum thickness Reynolds number). In a structured code where the grid lines are organized orthogonal to the wall a search algorithm can be used to find non-local variables, such as the boundary layer edge or to integrate quantities such as the momentum thickness. This is not possible with modern CFD codes using unstructured meshes and scalable parallelisation. A modification to a low-Re turbulence model (low-Re Wilcox k-ω) based on local variables has been developed by Langtry and Sjolander (2002). This modification has been shown to yield good predictions of transition for attached and separated flows.

All simulations in this paper are based on the commercial CFD software package CFX-5, (Ansys CFX, 2001). Simulations have been carried out for different test cases with experimental heat transfer data. All simulations have been carried out on a series of at least three grids to test grid independence. The simulations with the SST model including the automatic switch of the wall function are compared to results of the standard k-ω model with wall functions and a two-layer near wall treatment. Deficiencies of the standard k-ω model and the two-layer near wall formulation for separated flows will be demonstrated. In all cases the SST model shows to be superior, as it gives more accurate predictions and is less sensitive to grid variations. These results are encouraging in view of heat transfer analyses in complex devices in gas turbines.

NUMERICAL METHOD

CFX-5 (Ansys CFX, 2001) uses an implicit finite volume formulation to construct the discrete equations representing the Navier-Stokes equations for the fluid flow. The grid which represents the flow domain can be unstructured and composed of hexahedra, tetrahedra, wedges, and pyramids. A coupled algebraic multi-grid solver is used to give robust solutions for the governing discrete equations. In the subsequent sections the SST turbulence model, the automatic neat wall treatment, and the transition model are described.

The SST Turbulence Model

The SST model combines the advantages of the k-ε and the k-ω model to achieve an optimal model formulation for a wide range of applications. For this a blending function F1 is introduced which is equal to one near the solid surface and equal to zero for the flow domain away from the wall. It activates the k-ω model in the near wall region and the k-ε model for the rest of the flow. By this approach the attractive near-wall performance of the k-ω model can be used without the potential errors resulting from the free stream sensitivity of that model. In addition, the SST model also features a modification of the definition of the eddy viscosity, which can be interpreted as a variable c_μ, where c_μ in the k-ε model is constant. This modification is required to accurately capture the onset of separation under pressure gradients. The modelled equations for the turbulent kinetic energy k and the turbulence frequency ω are as follows:

$$\frac{\partial \rho k}{\partial t}+\frac{\partial \rho U_j k}{\partial x_j}=\tilde{P}_k-\beta^*\rho\,\omega\,k+\frac{\partial}{\partial x_j}\left(\Gamma_k\frac{\partial k}{\partial x_j}\right) \quad (1)$$

$$\frac{\partial \rho \omega}{\partial t}+\frac{\partial \rho U_j \omega}{\partial x_j}=\frac{\alpha}{\nu_t}P_k-\beta\rho\,\omega^2+\frac{\partial}{\partial x_j}\left(\Gamma_\omega\frac{\partial \omega}{\partial x_j}\right)+(1-F_1)2\rho\,\sigma_{\omega 2}\frac{1}{\omega}\frac{\partial k}{\partial x_j}\frac{\partial \omega}{\partial x_j} \quad (2)$$

where the blending function F_1 is calculated from

$$F_1=\tanh(\arg_1^4) \quad (3)$$

$$\arg_1=\min\left(\max\left(\frac{\sqrt{k}}{\beta^*\omega y};\frac{500\upsilon}{y^2\omega}\right)\frac{4\rho\sigma_{\omega 2}k}{CD_{k\omega}y^2}\right) \quad (5)$$

$$CD_{k\omega}=\max\left(2\rho\,\sigma_{\omega 2}\frac{1}{\omega}\frac{\partial k}{\partial x_j}\frac{\partial \omega}{\partial x_j};1.0e^{-10}\right) \quad (6)$$

The turbulent viscosity is then calculated by

$$\mu_t=\min\left[\frac{\rho k}{\omega};\frac{a_1\rho k}{SF_2}\right] \quad (7)$$

with the constant $a_1 = 0.31$ and the blending function F_2 obtained from

$$F_2=\tanh(\arg_2^2) \quad (8)$$

$$\arg_2=\max\left(2\frac{\sqrt{k}}{\beta^*\omega y};\frac{500\upsilon}{y^2\omega}\right) \quad (9)$$

The coefficients, φ of the model are functions of F_1: $\varphi = F_1\varphi_1+(1-F_1)\varphi_2$, where φ_1, φ_2 stand for the coefficients of the k-ω and the k-ε model respectively:

σ_{k1}=1.176, $\sigma_{\omega 1}$=2.000, κ=0.41, α_1=0.5532, β_1=0.0750, β^*=0.09, c_l=10 (10)

σ_{k2}=1.000, $\sigma_{\omega 2}$=1.168, κ =0.41, α_2=0.4403, β_2=0.0828, β^* = 0.09

More details about the model and its performance have been reported by Menter and Esch (2002). In a recent NASA Technical Memorandum by Bardina et. al (1997) the SST model was rated the most accurate model in its class.

For the treatment of the energy equation near the wall, an algebraic formulation is required to link the temperature and the heat flux. The formulation of Kader (1981) is used:

$$\Theta^+ = \mathrm{Pr}\cdot y^+ \cdot e^{-\Gamma} + \left[2.12\ln(1+y^+) + \beta(\mathrm{Pr})\right] e^{-1/\Gamma} \quad (11)$$

where

$$\beta(\mathrm{Pr}) = (3.85\,\mathrm{Pr}^{1/3} - 1.3)^2 + 2.12\ln(\mathrm{Pr}) \quad (12)$$

and

$$\Gamma = \frac{0.01(\mathrm{Pr}\cdot y^+)^4}{1+5\mathrm{Pr}^3\cdot y^+} \quad (13)$$

The non-dimensional temperature is defined as

$$\Theta^+ = \frac{T_w - T}{T_\tau};\quad T_\tau = \frac{q_w}{\rho c_p u_\tau} \quad (14)$$

Near Wall Treatment

It is generally accepted that the integration of the boundary layer through the thin viscous sub-layer near the wall is preferable to the use of wall function boundary conditions. The challenge is, however, that a strict low-Reynolds number model requires a very fine grid resolution. This requirement can hardly be achieved for all walls in complex geometries. It would also lead to excessive cell aspect ratios, which in most cases would require a double precision computation, thereby doubling the memory consumption of the code. If the grid is too coarse, the use of a low-Re model will result in a poor prediction. It is therefore desirable to offer the user a formulation that will automatically switch from wall functions to a low-Re formulation, as the grid is refined.

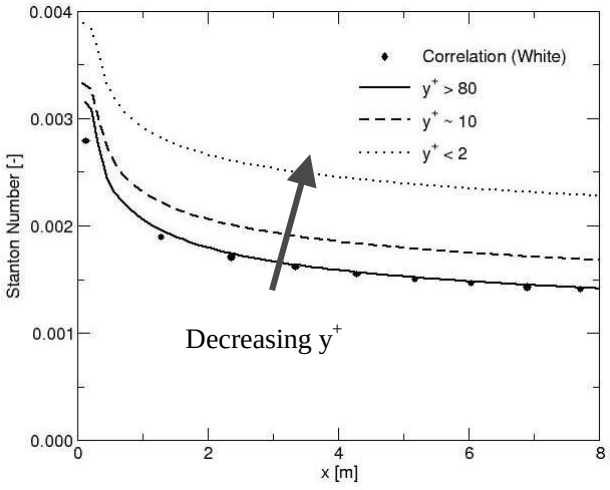

Figure 1: Grid sensitivity for standard wall functions

Figure 1 shows results for a simulation of the heat transfer along a flat plate on three different grids using the standard wall function approach. Clearly visible is the strong grid dependence of the results: The solution for the standard wall function deteriorates on the fine grids. The opposite behavior can be observed for the same simulation using a standard low-Re approach. In this case the solution deteriorates on coarser grids (Figure 2).

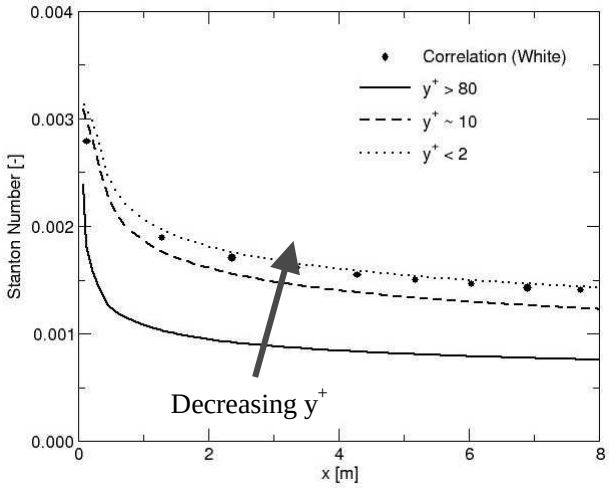

Figure 2: Grid sensitivity for standard low-Re treatment

The k-ω based models, including the SST model, have the advantage that an analytical expression is known for ω in the viscous sub-layer and the logarithmic region, which can be exploited to achieve the aforementioned goal. The basic idea is to blend the wall value of ω between the logarithmic and the low-Re formulation. While in the wall function formulation the near wall grid point is treated as being outside the edge of the viscous sub-layer, the location of the near wall grid node is virtually moved down through the viscous sub-layer as the grid is refined in the low-Re mode.

This new wall boundary condition has been implemented in combination with the SST model (Grotjans and Menter, 1998). It exploits the simple and robust near wall formulation of the underlying k-ω model and switches automatically from a low-Reynolds number formulation to a wall function treatment based on the grid density. The advantage is that the user can make optimal use of the advanced performance of the turbulence model, for a given grid. The automatic wall treatment avoids the deterioration of the results typically seen if low-Re models are applied on under-resolved grids.

A blending function depending on y^+ is used. The solutions for ω in the linear and the logarithmic near-wall region are:

$$\omega_{Vis} = \frac{6\nu}{0.075 y^2};\quad \omega_{\log} = \frac{1}{0.3\kappa}\frac{u_\tau}{y} \quad (15)$$

They can be re-formulated in terms of y^+ and a smooth blending can be performed:

$$\omega_1(y^+) = \sqrt{\omega_{Vis}^2(y^+) + \omega_{\log}^2(y^+)} \quad (16)$$

A similar formulation is used for the velocity profile near the wall:

$$u_\tau^{Vis} = \frac{U_1}{y^+};\quad u_\tau^{\log} = \frac{U_1}{\frac{1}{\kappa}\ln(y^+) + C} \quad (17)$$

with

$$u_\tau = \sqrt[4]{(u_\tau^{Vis})^4 + (u_\tau^{\log})^4} \quad (18)$$

This formulation gives the relation between the velocity near the wall and the wall shear stress. For the k-equation, a zero flux

boundary condition is applied, as this is correct for both the low-Re and the logarithmic limit. For the energy equation, the formulation given by Eq. (11) is used.

Compared to the standard wall-function or the low-Re approach it is clearly visible that the grid dependency of the results for the automatic wall treatment is significantly reduced compared to the standard low-Re formulation (Figure 3). Figure 4 shows the impact of the grid resolution on the velocity profile close to the wall.

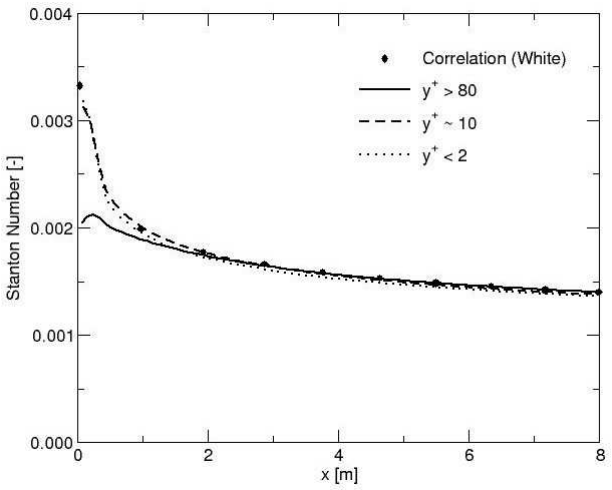

Figure 3: Grid sensitivity for the new automatic wall treatment

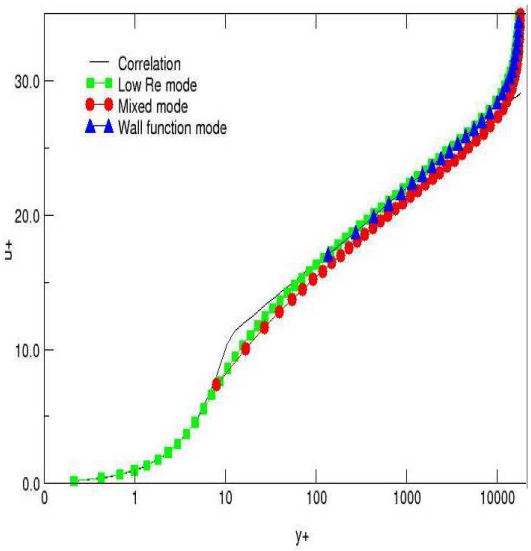

Figure 4: Velocity profiles based on automatic wall treatment for three different grids (square: viscous sublayer grid with y^+~0.1, circle: buffer layer grid with y^+~8, triangle: log-law grid with y^+~100)

Transition Modelling

The location of the start and the extension of transition are of major important in the design and performance of many technical devices, where the wall-shear-stress or wall heat transfer is of interest. The SST model was originally developed for fully turbulent flows. As a result, a few modifications must be made so that it will be compatible with the presence of a laminar boundary layer in the flow (Langtry and Sjolander, 2002). The SST model must be modified as follows. Eq. (7) for the turbulent viscosity is

$$\mu_t = \min\left[\alpha^* \frac{\rho k}{\omega}; \frac{a_1 \rho k}{\Omega F_2}\right] \qquad (19)$$

where α^* has only an impact in the low-Re region and the constants of set 1 (φ_1) are change to following values instead of their original SST values:

$$\alpha_1^* = \frac{\alpha_o^* + R_T / R_k}{1 + R_T / R_k} \qquad \alpha_1 = \frac{5}{9} \cdot \frac{\alpha_o + R_T / R_\omega}{1 + R_T / R_\omega}$$

$$\alpha_2^* = 1.0 \qquad \alpha_0^* = 0.025$$
$$\alpha_2 = 0.4403 \qquad \alpha_0 = 0.1$$

$$\beta_1^* = 0.09 \cdot \frac{5/18 + \left(R_T / R_\beta\right)^4}{1 + \left(R_T / R_\beta\right)^4} \qquad (20)$$
$$\beta_2^* = 0.09$$

$R_k = 6 \quad R_\omega = 2.7 \quad R_\beta = 8$

The transport equation for the turbulent kinetic energy Eq. (1) includes a modification that takes transition into account as follows:

$$\frac{D\rho k}{Dt} = P_k PTM - \beta^* \rho \omega k + \frac{\partial}{\partial x_j}\left((\mu + \sigma_k \mu_t)\frac{\partial k}{\partial x_j}\right) \qquad (20)$$

The production term P_k for k is calculated from

$$P_k = \min\left(P_{korig}; \mu_t \Omega^2\right) \qquad (21)$$

where P_{korig} is the original strain-based production term from the SST model

The modified blending function F_1 is defined as

$$F_1 = \max\left(F_{1orig}; F_4\right) \qquad (22)$$

where F_{1orig} is the original blending function as defined by Eq. (3) and F_4 is given by

$$F_4 = \exp\left[-\left(\frac{R_y}{120}\right)^8\right] \qquad (23)$$

The PTM term in Eq. (20) that is used to control the production of k in a laminar boundary layer takes the following form:

$$PTM = 1 - \left[0.94\left(PTM_1 + PTM_2\right)\right]F_3 \qquad (24)$$

The PTM term can vary from 0 to 1, where 1 would result in the fully turbulent term. PTM_1 accounts for the effects of freestream turbulence intensity and PTM_2 is a function of the pressure gradient.

The F_3 term is a switching function that disables the model outside of laminar boundary layers and allows a smooth blending between the laminar region and the transitional region. The most obvious choice for the dependent variable is the viscosity ratio ($R_T = \rho k/(\omega\mu)$). Based on the work of Biswas and Fukuyama (1994) and some numerical experimentation, F3 is defined as follows:

$$F_3 = \exp\left[-\left(\frac{R_T}{5.0}\right)^4\right] \qquad (25)$$

The PTM_1 term is calibrated such that the model correctly reproduces the effect of freestream turbulence intensity on the transition onset location in zero pressure gradients.

$$PTM_1 = \begin{cases} 1-\left[\begin{matrix} 3.82\times10^{-4}\,\mathrm{Re}_V - 3.94\times10^{-7}\,\mathrm{Re}_v^2 \\ +1.43\times10^{-10}\,\mathrm{Re}_v^3 \end{matrix}\right], \mathrm{Re}_v < 1000 \\ 1-\left[0.12+1.0\times10^{-5}\,\mathrm{Re}_V\right], \mathrm{Re}_v \geq 1000 \end{cases} \quad (26)$$

The final proposed form for the PTM_2 term, arrived at by numerical experimentation in Langtry and Sjolander (2002), is as follows:

$$PTM_2 = \begin{cases} -|K|^{0.4}\,\frac{\mathrm{Re}_V}{80}, K < 0 \\ 0, K \geq 0 \end{cases} \quad (27)$$

The pressure gradient parameter K is defined as follows:

$$K = -\frac{\mu}{\rho^2 U^3}\left[1-M^2\right]\frac{dp}{ds} \quad (28)$$

where dp/ds is the pressure gradient along the local streamline and U is the local resultant velocity.

RESULTS AND DISCUSSION

The SST model in combination with the improved near wall treatment have been validate in a series of test cases; see for example Esch and Menter (2002). In the present analysis validation cases are used that are typical for heat transfer in gas turbines.

Case 1: Pipe Expansion

The flow being modelled is the incompressible flow in a pipe expansion. Downstream of the expansion, the pipe is heated with a uniform heat flux. From the experiments, the local Nusselt number distributions for various Reynolds numbers are known. The experiments were carried out by Baughn et a. (1984).

Figure 5 shows the geometry of the pipe expansion. The inlet is placed one-step height, H, upstream of the step. The outlet boundary is located 40 H downstream of the step. The expansion ratio is d/D = 0.4. The Reynolds number, based on H and the mean inflow velocity, is Re_H=20,000. The inflow conditions for velocity and turbulence were specified using profiles for fully turbulent pipe flow, which were calculated in separate simulations.

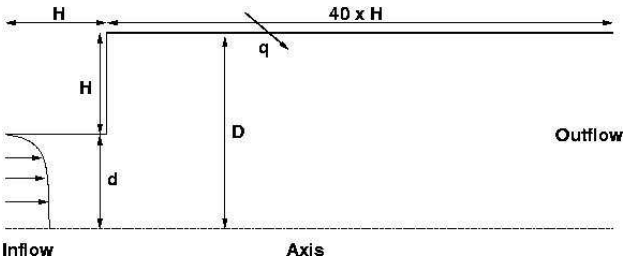

Figure 5: Domain for the turbulent flow in a pipe expansion

Figure 6 compares the predicted Nusselt number distributions of the SST and k-ε two-equation and a k-ε two-layer turbulence model. It can be seen from the results that the two-equation models capture the location of the Nusselt number peak in good agreement with the experimental data. The k-ε model over-predicts the peak Nusselt number by about 20%, whereas the SST results are within 5% of the measured values but show a slightly broader distribution near the maximum Nusselt number than the other turbulence models.

For comparison reason also results of a two-layer turbulence model are shown. The two-layer turbulence model combines the standard high-Re k-ε model with the one-equation model of Yap in the viscous sub-layer. The two-layer model strongly under-predicts the Nusselt number over most of the domain, although the y^+ were well below '1' for the finest grid. Bredberg et al. (2000) report a similar behaviour and attribute this to the "faulty length-scale representation".

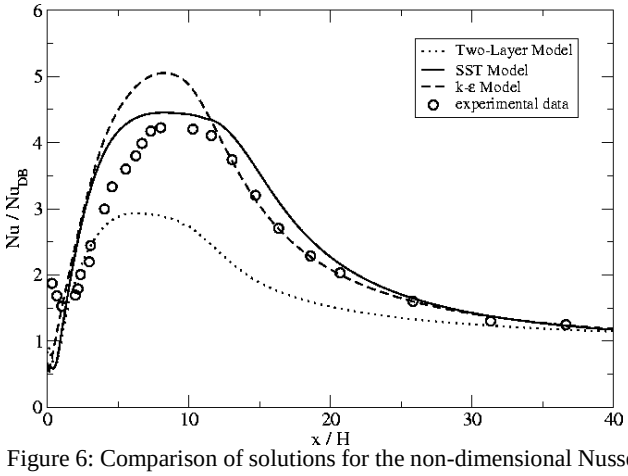

Figure 6: Comparison of solutions for the non-dimensional Nusselt number distribution along the outer pipe diameter.

Case2: 2D-Rib

The second test case considered is the incompressible flow in a rectangular channel with ribs mounted on one of the duct walls. The flow is representative of the flow between cooling-ribs in gas turbines. The flow field is assumed periodic in the streamwise direction, so that only one rib is modelled and periodic boundary conditions (except for pressure and temperature) are applied between the upstream and downstream boundaries. From the experiments, the local Nusselt number distributions along the lower and upper walls are known. The experiments were carried out by Nicklin (1998).

Figure 7 shows the geometry of the rib-roughened channel. The height and width of the domain is 10 times the rib height, e.

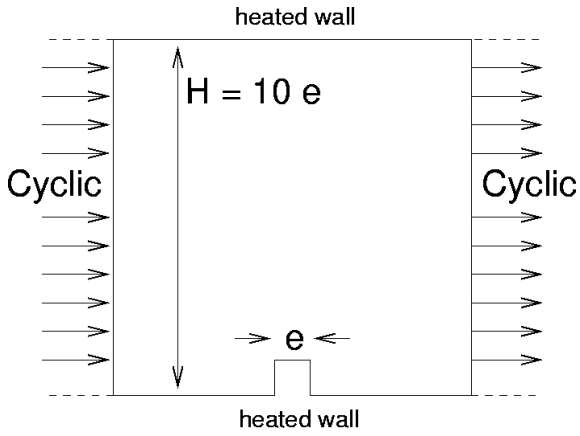

Figure 7: Domain for the rib-roughened 2D channel

The upper and lower walls, including the rib were modelled using viscous heat flux specified walls. The heat flux was set to 5×10^{-2} Wm^{-2}. The left and right boundaries were coupled by periodicity, except for the pressure and temperature field. The pressure and temperature gradients have to be found iteratively. Both values have to be readjusted for each grid until vanishing

global momentum and energy balances are achieved.

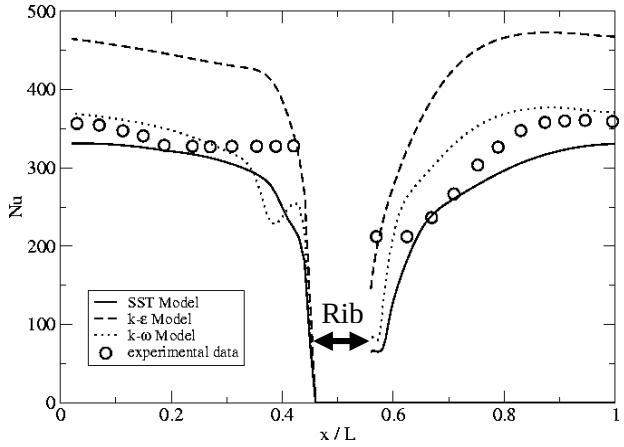

Figure 8: Nusselt number distribution on the lower wall of the channel; Re_H=100,000

To evaluate the accuracy of the turbulence models the Nusselt number distribution on the lower wall, including the rib, was evaluated as Nu(x)=h(x)H/k. A comparison of the tested two-equation models shows that the closest agreement with the experimental data is obtained with the SST and k-ω models. The k-ε model predicts the general trend but overestimates the heat transfer upstream and downstream of the rib by about 30% (Figure 8).

Case 3: Nozzle Guide Vane

The blade used here is a stator guide vane with incompressible flow from Ubaldi et al (1996). The grid used for the numerical simulations had approximately 40,000 nodes and an average y^+ value of 1. The inflow Mach number for the case was 0.24 and the Reynolds number based on outlet flow conditions and chord length was 1.6×10^6. The free stream turbulence intensity at the blade leading edge was 1%. It shows transitions at mid chord on the suction side and the pressure side is fully laminar. Shown in Figure 9 are contour plots of turbulence intensity around the blade, which clearly indicate that turbulent flow is only found after mid chord on the suction side.

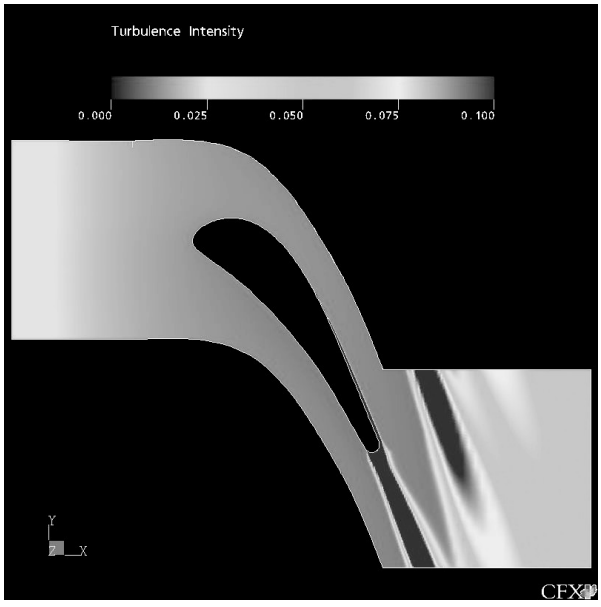

Figure 9: Turbulence Intensity, where dark colour represents high level of turbulence intensity.

Figure 10 shows friction velocity (u_*/U_o) along the axial chord line using the transition model. It captures accurately the experimental data. For this case there are no heat transfer data available; however, a model that assumes fully turbulent flow over the complete chord length would over predict the high heat transfer rate.

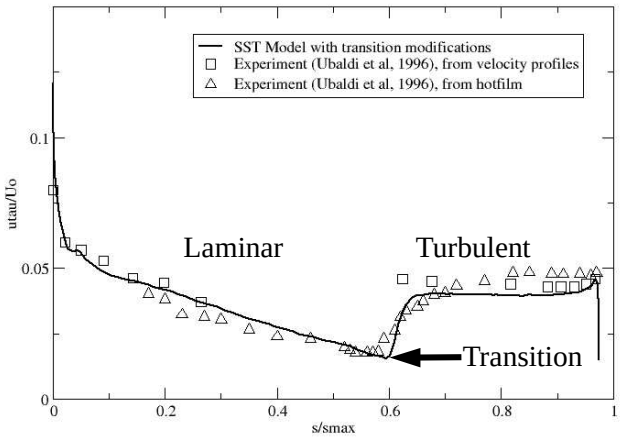

Figure 10: Suction side normalised friction velocity distribution along the axial chord length

SUMMARY

The SST model has been applied with an automatic wall treatment, which switches automatically between wall functions and a low-Re treatment based on the grid spacing. It was demonstrated that both near wall formulations lead to a significant reduction in the sensitivity of heat transfer predictions to the near wall resolution. This is an essential feature of all turbulence models in CFX-5. The low sensitivity to the grid spacing is important for industrial flow predictions, where typically not all walls can be resolved with fine grids. Both formulations remove the necessity to place the first grid point into the logarithmic region of the velocity profile.

Best overall agreement for all test cases was achieved with the SST-model making it an excellent choice for heat transfer predictions. It was observed in all simulations, that great care is required to properly set up heat transfer test cases. It is important that a sufficiently fine grid is employed and that all boundary conditions are carefully set up in agreement with the experimental data.

ACKNOWLEDGEMENTS

The authors wish to thank General Electric for financial support of parts of the analyses and Robin Langtry for implementing the transition model in the CFX software.

BIBLIOGRAPHIC REFERENCES

Abu-Ghannam, B.J. and Shaw, R., 1980, " Natural transition of boundary layers - the effects of turbulence, pressure gradient and flow history". *J. of Mechanical Engineering Science*, Vol. 22, pp. 213 - 228.

ANSYS CFX, 2001, CFX-5 Documentation.

Arts, T., 1991, Data available via ERCOFTAC special interest group: (http://www.mecaflu.ec-lyon.fr/CONGRES/ERCOFTAC/database/register.html).

Bardina, J.E., Huang, P.G., Coakley, 1997, T.J. "Turbulence Modeling Validation, Testing, and Development", NASA Technical Memorandum 110446.

Baughn, J.W., Hoffmann, M.A., Takahashi, R.K. and Launder, B.E., 1984, "Local Heat Transfer Downstream of an Abrupt Expansion in a Circular Channel With Constant Wall Heat Flux",

Vol. 106, Journal of Heat Transfer, pp. 789 – 796.

Biswas, D. and Fukuyama, Y., 1994, "Calculation of Transitional Boundary Layers With an Improved Low-Reynolds -Number Version of the k-ε Turbulence Model," *Journal of Turbomachinery*, Vol. 116, pp. 765-773.

Bredberg, J., Davidson, L. and Iacovides, H., 2000, "Comparison of near-wall behavior and its effect on heat transfer for k-ε and k-ω turbulence models in rib-roughened channels". In Nagano,. Y., Hanjalic, K., and Tsuji, T. eds: 3rd Int. Symposium on Turbulent Heat and Mass Tranfer, pp 381-388.

Craft, T. J., Graham, L. J. W., and Launder, B. E., 1993, "Impinging jet studies for turbulence model assessment – II. An examination of the performance of four turbulence models", *Int. J. Heat Mass Transfer*. 36(10), pp. 2685-2697.

Dol, H. and Hanjalic, K., 1997, " Development of a differential thermal second-moment closure using DNS data of the natural convection in a vertical channel". In Hanjalic, K. and Peeters, T.W.J.: *2nd Int. Symposium on turbulence, heat and mass transfer*, Delft University Press.

Grotjans, H., and Menter, F.R., 1998, "Wall functions for industrial applications". In K.D. Papailiou, Editor, *Computational Fluid Dynamics'98*, Volume 1, Part 2, pp 1112-1117, Chichester. ECCOMAS, John Wiley Sons.

Jones, W.P. and Launder B.E., 1972, "The prediction of laminarization with a two-equation model of turbulence". *International Journal of Heat and Mass Transfer*, 15.

Kader, B.A., 1981, "Temperature and concentration profiles in fully turbulent boundary layers". Int. Journal of Heat and Mass Transfer, 24, pp 1541-1544.

Langtry, R. B. and Sjolander, S.A., 2002, "Prediction of Transition for Attached and Separated Shear Layer in Turbomachinery, AIAA-2002-3643

Leschziner, M.A., 1994, "Refined turbulence modelling for engineering flows". ECCOMAS '94 Conference, Stuttgart, Germany, John Wiley Sons, pp. 206-219.

Leschziner, M.A., Ince, N.Z., 1995, "Computational modelling of three-dimensional impinging jets with and without cross-flow using second-moment closure". *Computers & Fluids* Vol. 24, No. 7, pp. 811-832.

Mayle, R.E., 1991, "The role of laminar-turbulent transition in gas turbine engines". *Journal of Turbomachinery*, 113, pp 509-537.

Menter, F.R., 1992, "Influence of free stream values on k-ω turbulence model predictions". *AIAA Journal*, 30(6), pp 1657-1659.

Menter F.R., 1994, "Two-equation eddy-viscosity turbulence models for engineering applications". AIAA-Journal, 32(8), pp. 269-289.

Menter, F.R. and Esch, T. 2001, "Elements of industrial heat transfer predictions". *16th Brazilian Congress of Mechanical Engineering (COBEM)*, Nov. 2001, Uberlandia, Brazil.

Nicklin, G. J. E., 1998, "Augmented heat transfer in a square channel with asymmetrical turbulence production", Final year project report, Dept. of Mech. Eng., UMIST, Manchester.

Rodi, W., and Scheuerer, G., 1986, "Scrutinizing the k–ε turbulence model under adverse pressure gradient conditions". *J. Fluids Eng.* 108.

Savill, A.M., 1993, "Some recent progress in the turbulence modelling of by-pass transition". In: R.M.C. So, C.G. Speziale and B.E. Launder, Eds.: Near-Wall Turbulent Flows, Elsevier, p. 829.

Ubaldi, M., Zunino, P., Campora, U., and Ghiglione, A., 1996, "Detailed velocity and turbulence measurements of the profile boundary layer in a large scale turbine cascade". *ASME paper no. 96-GT-42, 1996*.

Viegas, J.R. and Rubesin, M.W. 1983, "Wall-function boundary conditions in the solution of the Navier-Stokes equations for complex compressible flows". AIAA-83-1694.

Wilcox, D.C., 1993, "Turbulence Modeling for CFD". DCW Industries, Inc., La Canada, CA.